Automatic hippocampal multimodal assessment for studies of stroke and small vessel disease

Maria del C. Valdés Hernández[1]
M.Valdes-Hernan@ed.ac.uk
Jaeil Kim[2]
threeyears@kaist.ac.kr
Ian Whitteford[3]
s1104030@sms.ed.ac.uk
Xinyi Qiu[3]
s1108147@sms.ed.ac.uk
Joanna M. Wardlaw[1]
Joanna.Wardlaw@ed.ac.uk
Jinah Park[2]
jinahpark@kaist.ac.kr

[1] Brain Research Imaging Centre
University of Edinburgh
Edinburgh, UK

[2] Department of Computer Science
Korea Advanced Institute of Science and Technology,
Daejeon, South Korea

[3] College of Medicine and Veterinary Medicine
University of Edinburgh
Edinburgh, UK

Abstract

We propose a framework for assessing the hippocampi on stroke patients and studies of small vessel disease, where sclerosis, perivascular spaces and infarcts on this structure are common. It includes hippocampal and cavity segmentations, hippocampal shape modelling, feature characterisation and statistical analyses, all which have been particularly developed for assessing extreme abnormalities on this small brain structure on clinical MRI datasets. The hippocampal segmentation uses FSL™ tools. We apply this approach to 48 datasets from a study of mild stroke and assess its relevance on a larger dataset of 189 stroke patients. Using shape similarity metrics we show that the hippocampal shape models generated by our method are accurate on this dataset. We estimate the prevalence and distribution of the features analysed on the samples to discuss the usefulness of our approach.

1 Introduction

The temporal lobe and, in particular, the hippocampus play an important role in cognitive processes. Advanced magnetic resonance imaging (MRI) techniques combined with histology have confirmed the presence of markers of small vessel disease in the hippocampus such as microinfarcts and perivascular spaces [1]. Some of them may represent a diffuse vascular process with adverse local effects and/or proxies for larger volumes of infarcts or mild or severe diffuse damage [2]. They appear as cavities of circular or ovoid shape hyperintense in axial T2-weighted [1] and, if >=2-3 mm diameter, hypointense in axial fluid attenuation inversion recovery (FLAIR) MRI sequences. In

addition, hippocampal sclerosis occurs in substantial number of older persons. It visually reduces the hippocampal size and causes extreme deformations in its shape.

We developed computational methods for quantitatively assessing hippocampal cavities and hippocampal shape deformities, and integrated them on a framework that gives as output a full characterisation of these structures ready to be used in statistical analyses.

2 Methods

2.1 Preprocessing

Hippocampi were segmented from T1-weighted volume scans using an atlas-based segmentation approach based on FSL FLIRT and FAST [3], and an ageing template generated in-house from 97 brains of Caucasian individuals aged 65-70 years old. The generated hippocampal binary masks were all visually inspected and manually rectified using Analyze 12.0^{TM}. FLAIR hypointensities in the hippocampi, of >=2mm diameter with circular or oval shapes, were, separately, semi-automatically masked also using the same software. They correspond to hyperintensities in T2-weighted and have been reported as small cavities [1]. Results were overseen by a trained image analyst and a neuroradiologist.

2.2 Hippocampal shape modelling

We developed a shape modelling method tailored to small and highly-variable shape structures like the hippocampus, based on the Laplacian surface deformation framework, proposed by Kim and Park [4]. This method is characterised by a non-rigid template deformation in a coarse-to-fine style to minimise the distortion of the point distribution of the template surface model during the target surface reconstruction. It encodes the point distribution of the template surface model as Laplacian coordinates representing the relative positions of each point with respect to the average position of their neighbours and preserves the Laplacian coordinates of the template model as rigid as possible to sample the target surface with the point distribution of the template model. Consequently, the preservation of this point-wise correspondence allows us to make comparative analyses on shape variations.

From the binary hippocampal masks of the sample, mean shape images are constructed via an iterative and non-linear image registration between the binary masks following the process described in [5]. From the mean shape images, the template surface models for left and right hippocampi are, then, generated as triangular meshes using spherical harmonics following by a point distribution model (SPHARM-PDM v1.11) [6]. Further, to recover each individual shape, the template models are rigidly aligned to each target volume (i.e. left and right hippocampal binary masks) via the iterative closest point algorithm [7], following non-rigid deformation. Under the definition of Laplacian coordinates as the difference between each point's position and the centre of mass for their neighbouring points, the surface $\overline{\mathbf{V}}$ of the non-rigid template deformation is formulated as a quadratic form (equation (1)).

$$\overline{\mathbf{V}} = \underset{\mathbf{V}'}{\operatorname{argmin}} \left(\left\| \alpha \left(\mathbf{LV}' - \mathbf{LV} \right) \right\|^2 + \sum_{1}^{n} \left\| b_i - v_i \right\|^2 \right) \quad (1)$$

where $\mathbf{V}$ is the set of all vertices v_i for the points (each point denoted as i), α is a weighting term that controls the rigidity of the deformable model, L is a discrete Laplacian operator and b_i is the closest image boundary on the surface normal at each point, defined as:

$$b_i = \beta \cdot \left(m_i - v_i \right) + v_i \quad (2)$$

where m_i is the closest image boundary on the direction normal to the vertex and β is a weighting term introduced to regularise the vertex transformation.

In order to preserve the Laplacian coordinates as rigid as possible, we employ a progressive weighting scheme for α as described in [4]. Under this scheme, the template surface model is deformed with as-large-as-possible α values until the points of the template model best fit the boundary. This iterative process decreases α in a stepwise way, together with the magnitude of the displacement of each vertex. We experimentally determined that the maximum α value for our purpose was equivalent to 10 times the volumetric ratio between template and target. The optimal $\mathbf{V}$ for equation (1) can be obtained by solving a linear system using a matrix form of the Laplacian operator via a linear least squares approach. The solution is described in detail elsewhere [4].

We added the rotation and scale invariant (RSI) transformation proposed by [8] to the modelling process described in [4]. It constrains the vertex transformations only to rotation, isotropic scale and translation. This helps regularising the individual vertex transformation, derived by external factors, to the transformations of the neighbour vertices using them as reference.

2.3 Analyses of shape and cavities

A shape deformity map from the individual surface models is generated using the mean surface models of left and right hippocampi. The individual surface models are normalised via an isotropic rescaling of each shape model using hippocampal size and the generalised Procrustes analysis [9]. Local shape differences are determined by the displacement vectors between the corresponding vertices of the individual surface models and the mean surface model. The shape deformity at each vertex is computed as the signed Euclidean norm of the displacement vectors, projected on the vertex normal on the mean surface model to determine the direction of local shape changes.

The number of hippocampal cavities (i.e. hippocavities) and their load per hippocampi are derived automatically by assessing the intersection between the hippocavities mask and the hippocampal binary masks after a "fill-hole" operation is performed. The count was determined by counting the isolated clusters of hippocavities on each hippocampal mask. The load per structure is the total relative hippocavity volume of all hippocavities within a hippocampus. The morphology of individual hippocavities is quantified by its volume, maximum in-plane extent, roundness and sphericity. The "clusterisation" of small individual hippocavities is determined through the assessment of "compactness" as defined by Bibriesca in [10].

3 Experiments and Results

3.1 Datasets

We used MRI data from patients with lacunar or mild cortical stroke that presented with stroke symptoms to a teaching hospital between 2002 and 2013 and formally consented to participate on studies of stroke. All MRI data were acquired on the same 1.5T GE Signa Horizon HDxt clinical scanner operating in research mode with a self-shielding gradient set with maximum gradient of 33 mT/m, and an 8-channel phased-array head coil.

From a sample of 48 patients (14 women) mean age 66 (SD=10) years, we assessed the hippocampi and cavities as explained previously. To generate hippocampi binary masks we used T1-weighted spin-echo MRI scans of which 6 had matrix dimensions of 256x216x256 and voxel size of 1.0156x0.9x1.0156 mm^3 and the rest had matrix dimensions of 256x256x42 and voxel size of 0.9375x0.9375x4 mm^3. Cavities were assessed using FLAIR and T2-weighted images, only on 42/48 subsets in which images had matrix dimensions of 256x256x42 and voxel size of 0.9375x0.9375x4 mm^3. In the rest (i.e. 6/48 datasets), these sequences had very anisotropic voxels (0.4688x0.4688x6 mm^3) that were unsuitable for this purpose.

We visually assessed the presence of hippocavities on T2-weighted and FLAIR MR images from 189 MRI datasets from patients with acute lacunar ischaemic stroke clinical syndrome and a relevant lesion visible on the diffusion-weighted image, to examine their prevalence, appearance and distribution.

3.2 Results of the analyses of hippocampal shape and cavities on a subset of 50 stroke patients

In the shape modelling, β was set at 0.3 and α was progressively reduced from 30 to 1. For the 6 datasets with nearly isotropic voxels, β=0.5 and minimum α=0.3 were preferred, but for cross-evaluation purposes the results obtained with these α and β values were discarded. We visually checked the results using the MITK Workbench 2013.06.00 (Figure 1(a)) and calculated three similarity measures to quantitatively evaluate the modelling results (Table 1).

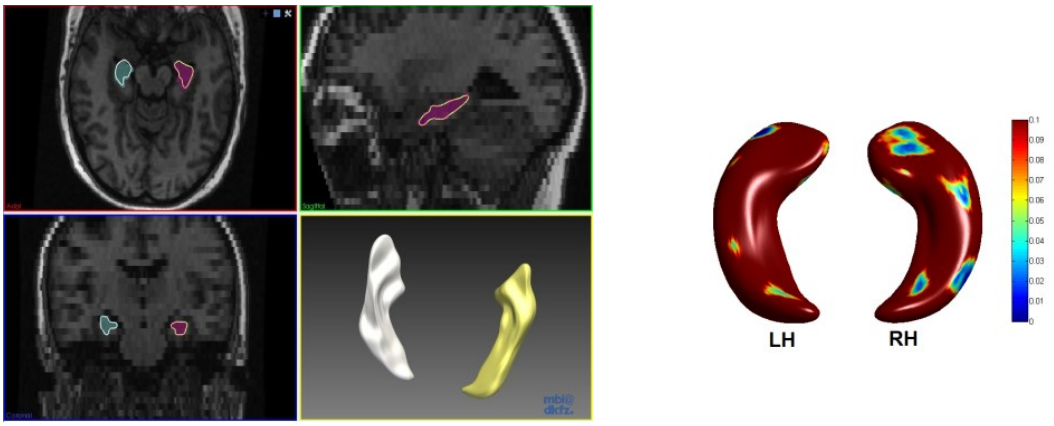

Figure 1: Illustration of results obtained from the shape analysis: Screenshot of the hippocampi shape models (superimposed onto the binary masks and the T1-weighted image) for a subject (left), and regions of significant deformation differences between the hippocampi from patients that had cortical vs. lacunar stroke (pattern superimposed onto the mean shapes of left and right hippocampi) (right).

Measure	Right Hippocampus	Left Hippocampus
Dice coefficient	0.9135 (IQR 0.0338)	0.8867 (IQR 0.0342)
Hausdorff distance (mm)	4.6482 (IQR 3.3304)	7.8551 (IQR 2.5206)
Mean distance (mm)	0.2006 (IQR 0.1711)	0.3595 (IQR 0.2450)

Table 1: Median and interquartile range values of the shape similarity measurements between the surfaces of the individualised (i.e. fitted) shape models and the hippocampal binary masks (after converting the latter to voxel meshes).

FLAIR hypointensities with intensity level 0 were found in 9/42 datasets, of which in 4/9 were single voxels. In general, single voxel FLAIR hypointensities, were found in 14/42 datasets, either scattered within the structure or in its periphery, or distributed in a line along the Cornu Ammonis 1 (dorsal hippocampi). Multivoxel structures of a single intensity value (of which 21 were elongated and 24 were ovoid) appeared on 25/42 datasets. Multivoxel structures of different intensity and shape patterns appeared on 37/42 datasets (Figure 2). The maximum hippocavity volume found was 49.22 mm^3 (ovoid shape).

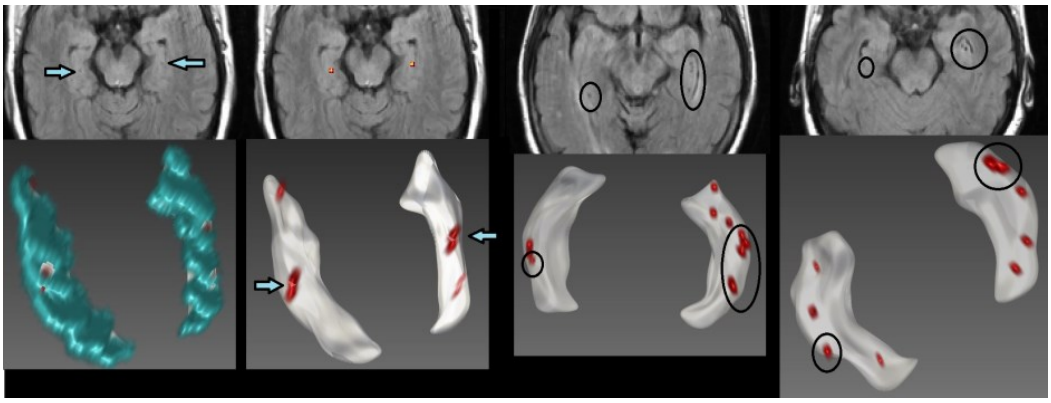

Figure 2: Three examples of the distribution of FLAIR hypointensities/T2-weighted hyperintensities on representations of their respective hippocampi. Arrows point to hippocavities penetrating the hippocampi. Encircled are hippocavities on the surface. The blue surface is the 3D representation of the binary mask.

3.3 Incidence of hippocampal cavities on a large sample of patients with lacunar stroke

Hippocavities were observed on 86/99 patients with the index stroke lesion in the left (L) cerebral hemisphere, on 67/78 patients with the index stroke in the right (R) cerebral hemisphere and, in general, on 82% of the sample (155/189), with a median value of 2 cavities per hemisphere regardless of the location of the index stroke. Only on two patients a hippocavity ovoid in shape with maximum diameter of 3-4 mm was observed. The rest were either round with 1-2 mm diameter or elongated small structures coincident with the appearance of perivascular spaces [11].

4 Discussion and Conclusion

An integrated framework that includes shape modelling and cavity characterisation for the assessment of the hippocampus on clinical MRI datasets of stroke patients and patients with small vessel disease has been proposed here. The anisotropy of the imaging voxels, extreme structural deformations and prevalence of several abnormalities imposed a manual

editing step for obtaining hippocampal binary masks and cavities. The rest of the process was fully automatic. The shape modelling pipeline presented, preserved the individual shape details allowing the detection of morphological changes of this structure. Further work will involve 1) evaluating its robustness against other state-of-the-art shape modelling methods and on detecting subtle morphological changes of this structure and 2) combining the hippocampal and cavity masks using the latter as a constraint on the deformation process.

Not all FLAIR hypointensities computationally identified by thresholding had the characteristics of those visually identified as hippocavities on the larger clinical sample. However, with the proposed framework, these could be identified. The prevalence and characteristics of those identified as possible hippocavities on the sample computationally analysed were in agreement with the visual assessment on the larger sample and with existent clinical reports [1,2].

Acknowledgements

This work was funded by Row Fogo Charitable Trust, the National Research Foundation of Korea (Grant no. 2012K2A1A2033133/no.2011-0009761) and the College of Medicine and Veterinary Medicine at the University of Edinburgh, UK.

References

[1] S.J. van Veluw, L.E.M. Wisse, H.J. Kuijf *et al*. Hippocampal T2 hyperintensities on 7 Tesla MRI. *NeuroImage:Clinical*, 3:196-201, 2013.

[2] Z. Arvanitakis, S.E. Leurgans, L.L. Barnes *et al*. Microinfarct pathology, dementia, and cognitive systems. *Stroke*, 42 (3):722-727, 2011.

[3] B. Patenaude, S. Smith et al. FMRIB Technical Report TR07BP1. Oxford, 2007.

[4] J. Kim and J. Park. Organ shape modelling based on the laplacian deformation framework for surface-based morphometry studies. *J Comp Sci Eng*, 6:219-226, 2012.

[5] G. Heitz, T.Rohlfing, C.R. Maurer Jr. Statistical shape model generation using non rigid deformation of a template mesh. *Sig Proc* 1411-1421, 2005.

[6] M. Styner, I. Oguz, S Xu, et al. Framework for the Statistical Shape Analysis of Brain Structures using SPHARM-PDM. *Insight Journal. NIH Public Access*, (1071):242-250, 2006.

[7] P.J. Besl and H.D. McKay. A method for registration of 3D shapes. *IEEE Trans on Pattern Analysis and Machine Intelligence*, 14(2):239-256, 1992.

[8] O. Sorkine, D. Cohen-Or, Y Lipman et al. Laplacian surface editing. Proc. Of the 2004 Eurographics/ACM SIGGRAPH Symposium on Geometry Processing, 175-184, 2004.

[9] J.C. Gower. Generalized Procrustes Analysis. *Psychometrika*, 40:33-51,1975.

[10] E. Bribiesca. An easy measure of compactness for 2D and 3D shapes. *Pattern Recognition*, 41:543-554, 2008.

[11] J.M. Wardlaw, E.E. Smith, G.J. Biessels et al. Neuroimaging standards for research into small vessel disease and its contribution to ageing and neurodegeneration. Lancet Neurol, 12:822-838, 2013.